

Design of Hollow-Rotor Brushless DC Motor

Raja Nor Firdaus Raja Othman^{1,2}, Farina Sulaiman^{1,2}, Suhairi Rizuan^{1,2,3}, Kasrul Abdul Karim^{1,2},
Auzani Jidin^{1,2}, Tole Sutikno⁴, Norhisam Mison⁵

¹Faculty of Electrical Engineering, Universiti Teknikal Malaysia, Melaka, Malaysia

²Electrical Machine Design, Power Electronics and Drives Research Group, CeRIA, UTeM

³Electrical Technology Section, Universiti Kuala Lumpur-British Malaysian Institute, Malaysia

⁴Department of Electrical Engineering, Universitas Ahmad Dahlan, Yogyakarta, Indonesia

⁵Faculty of Engineering, Universiti Putra Malaysia, 43400 Serdang, Selangor, Malaysia

Article Info

Article history:

Received Feb 6, 2015

Revised Apr 22, 2015

Accepted May 4, 2016

Keyword:

BLDC motor
Finite element method
Hollow-rotor
Leakage flux circling

ABSTRACT

This paper discusses about design of hollow-rotor Brushless DC (BLDC) motor. A conventional BLDC motor has more leakage flux circling at the end of the permanent magnet that will limit torque. To overcome this problem, a new BLDC model known as hollow-rotor is proposed. The objective of this research is to design a hollow-rotor motor that will have higher torque density compared to conventional BLDC motor using Finite Element Method (FEM). In addition, performance analysis of the proposed hollow-rotor has also been carried out. For validation, the result of FEM is compared with the measurement result. It shows that, the simulation result has good agreement with the measurement result. For comparison, hollow-rotor shows higher torque density compared to conventional BLDC motor. As a conclusion, this paper provides guidelines and analysis in designing high torque hollow-rotor motor.

Copyright © 2016 Institute of Advanced Engineering and Science.
All rights reserved.

Corresponding Author:

Raja Nor Firdaus Raja Othman,
Faculty of Electrical Engineering, Universiti Teknikal Malaysia, Melaka, Malaysia
Hang Tuah Jaya, 76100 Durian Tunggal, Melaka, Malaysia.
Email: norfirdaus@utem.edu.my

1. INTRODUCTION

BLDC motor is widely used in many applications, especially for home appliances such as blender, fan, mixer and vacuum [1-2]. The rotor of a typical BLDC motor usually has permanent magnets. By using permanent magnet, no electrical energy is required to excite the field, thus increasing the efficiency, torque density and power density of the motor [3-4]. Many researchers had focused on improving the torque of BLDC motor. For instance, Gyu-Hong Kang *et al.* studied irreversible demagnetization of permanent magnet. This irreversible demagnetization characteristic is analyzed by rotor structure. In a BLDC motor, the reluctance torque strongly influences the torque characteristics. By considering these characteristics, the motor performance in terms of magnetic flux density will proportionally increase the torque [5-7]. Another example is the study by Byoung-Kuk Lee *et al.*, who presented a detailed comparative study of BLDC motor due to operating condition. In this study, flux barriers are design in order to improve torque characteristics. By using this method, magnetic flux will be concentrated in the air gap. As a result, flux barrier can maximize the torque of the BLDC motor compared to conventional types [8-10]. M.R. Mizanoor *et al.* presented an analytical model for calculating the back emf and the maximum value of air gap flux density in both radial and tangential directions for internal rotor topology. The flux density in the air gap region is derived by considering the stator slot opening [11-12]. Another researcher, K.W. Hyung *et al* proposed a method for optimizing torque for developing the neodymium free spoke type BLDC motor. An important step during motor design is the calculation of the effective air gap flux density. Effective air gap flux density is contributed from the flux of magnet [13]. In summary, most of the researchers increase torque by applying

a barrier or decrease the losses of the demagnetization effect. However, it will be better if a new method could be introduced to solve both problems. For such reason, magnetic flux below the permanent magnet is essential to minimize the leakage flux. The leakage flux does not contribute to the torque generation.

This paper presents design of hollow-rotor BLDC motor. Several design parameters for designing the conventional BLDC motor had been investigated. A new model known hollow-rotor is design to improve the performance for BLDC motor. Hollow-rotor motor is fabricated and the measurement result is compared with FEM. The result shows that simulation has shown good agreement with measurement result. The proposed hollow-rotor motor can be designed for higher rating of BLDC motor up to kW specification.

2. DESIGN OF CONVENTIONAL BLDC

2.1. Design of Stator and Coil

Before designing hollow-rotor, a conventional BLDC motor is design first. The stator and rotor design for conventional BLDC motor is shown in Figure 1. In this research, BLDC motor is design for 9 slot 8 pole arrangements. Investigation is made in order to properly design of stator and magnet volume with reasonable design parameter so that motor performance can be maximized. The rotor and stator is mostly covered by standard silicon steel grade as J1: 50H800. Futher details about design parameter are shown in table 1. At this stage, no permanent magnet is applied to the motor.

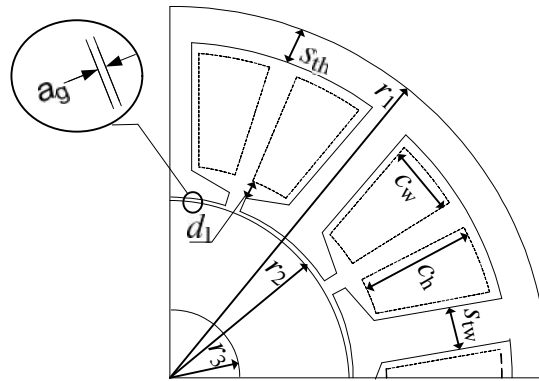


Figure 1. Stator and rotor design

The fixed parameter for designing BLDC motor is the stator radius r_1 , inner rotor radius r_2 , outer rotor radius r_3 , coil height c_h , coil width c_w , air gap a_g , distance slot opening d_1 . The varied parameter is the stator tooth height s_{th} which is change from 1 mm to 2 mm. Stator tooth width s_{tw} is change from 2 mm to 4 mm. Stator tooth width s_{tw} is change linearly with the change of s_{th} from 1 mm to 2 mm with the difference of 0.5 mm as shown in equation (1).

$$s_{th} = \frac{1}{2}(s_{tw}) \quad (1)$$

Number of turn, n is set from 26 until 10 accordingly to the coil size, c_s of coil slot space. The coil turn can be calculated by;

$$N = \left(\frac{c_w}{c_s} \right) \left(\frac{c_h}{c_s} \right) \times 70\% \quad (2)$$

Figure 2 shows selection of coil. Firstly, 3 set of models with different size of s_{tw} and s_{th} is been modeled. For each model, different number of turn is set based on equation (2). Firstly, coil, c_s is set 0.2 mm and current I is 2 A. Result for flux density is recorded. The procedure is repeat for c_s 0.4 mm until 1.0. Next, current is change to 4 A and 6 A and the procedure is repeated again. The entire model will be simulated by using Finite Element Method (FEM) with applied current 2 A until 6 A. Result for flux density at stator pole for

each model is recorded for analysis process. Figure 3 shows analysis result for flux density for all model. This analysis is done in order to choose coil size for winding purpose. The result of flux density is determine at stator pole when no magnet is applied in the model. Figure 3 (a) is flux density result for model A. Figure 3 (b) is flux density result for model B while figure 3 (c) is flux density result for model C. The entire model has the same value of flux density when coil sizes are set to minimum size 0.2 mm which is 2.2 T at 6 A, but when coil size is set to maximum value 1.0 mm, only model B and model C has the same value at maximum current of 6 A which is 0.8 T while model A is 1.3 T. When coil 0.6 mm is apply, the maximum stator flux density is near to 1.5 T for model A, B and C. For further analysis process, coil size of 0.6 mm is selected at maximum current 6 A, based on result for stator pole flux density for all three models where when using 0.6 mm coil, maximum flux density at stator pole will be from range 1.6 T to 1.75 T. Beside that, coil size 0.6 mm is the middle value for coil size range 0.2 mm to 1.0 mm.

Table 1. BLDC specification

Parameter		Value
Stator tooth height, s_{th}	[mm]	1,1.5,2
Stator tooth width, s_{tw}	[mm]	2,3,4
Stator radius, r_1	[mm]	25
Inner rotor radius, r_2	[mm]	12.4
Outer rotor radius, r_3	[mm]	3
Coil height, c_h	[mm]	2.5
Coil width, c_w	[mm]	7
Coil size, c_s		0.2,0.4,0.6,0.8,1.0
Air gap, a_g	[mm]	0.5
Distance slot opening, d_1	[mm]	1
Num of turn, N		262,65,29,16,10
Current	[A]	2,4,6

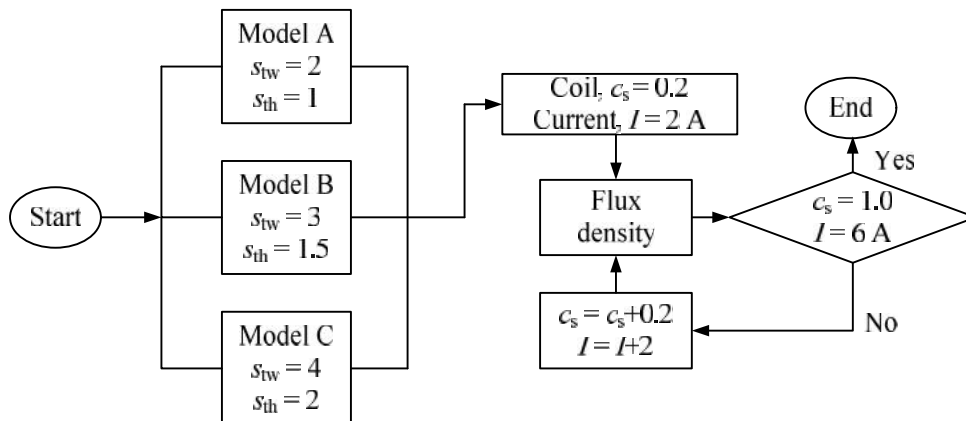
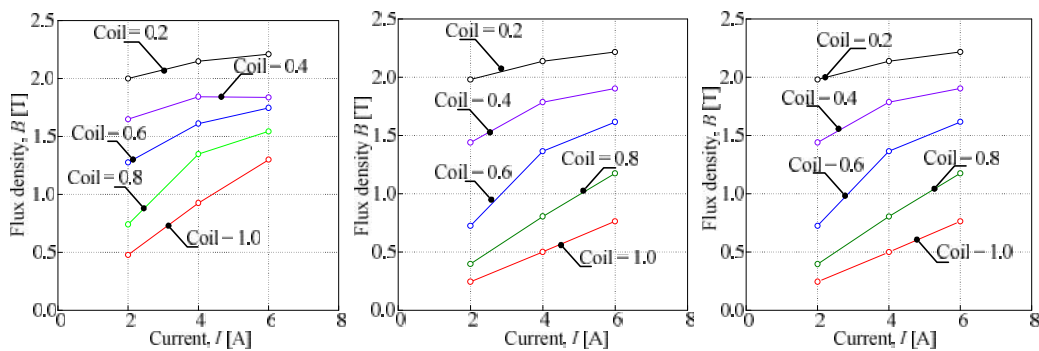


Figure 2. Selection of coil



(a) Stator pole flux density model A (b) Stator pole flux density model B (c) Stator pole flux density model C

Figure 3. Analysis result for stator and coil

2.2. Design of Permanent Magnet

For selecting the permanent magnet height, m_h is varied from 2 mm to 4 mm while magnet width m_w is set either 2 mm or 4 mm as shown in figure 4. Figure 5 shows selection of magnet volume. After suitable coil size is selected as shown in previous analysis, another analysis is conducted for selecting reasonable magnet volume. Selection of volume is from 160 mm² until 480 mm². Magnet is included in model A, B and C. The model is again simulated by using FEM. At this point, the source current will be set to zero so that result recorded for flux density will fully focus on permanent magnet energy.

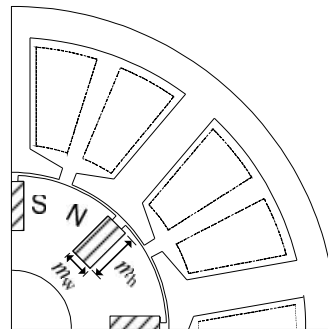


Figure 4. Permanent magnet design

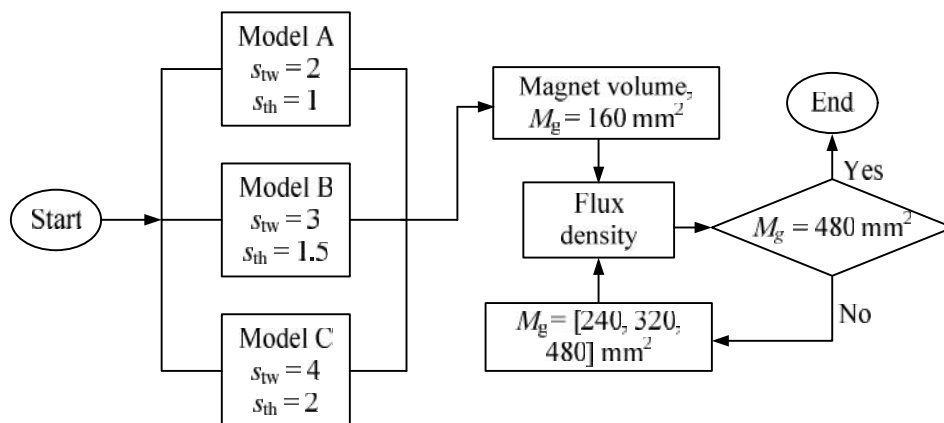


Figure 5. Selection of magnet volume

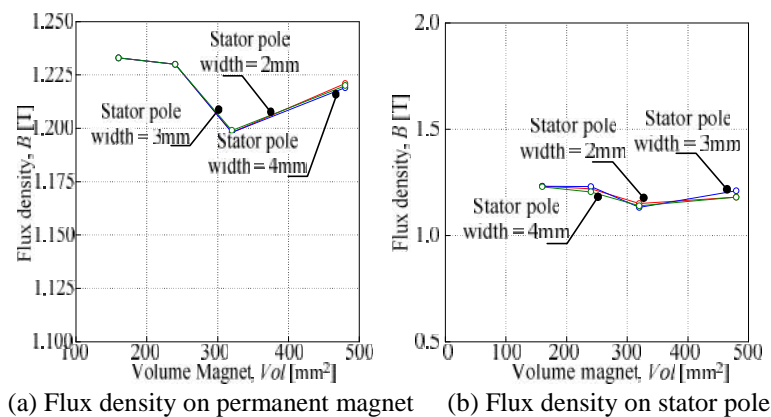


Figure 6. Analysis result for magnet volume

Figure 6 (a) shows magnet flux density for each model when different volume of magnet is inserted in rotor. The result is recorded when there is no current source. The flux density appears is due to permanent magnet energy. Maximum magnet flux density occurs when magnet volume is 160 mm² which is 1.23 T while minimum flux density occurs at magnet volume 320 mm² which is 1.2 T. All three models have the similarity increment and decrement point for all magnet volume. Figure 6 (b) shows result for stator pole flux density when magnet is included. During this process, there is current source included which is 6 A and number of turn N is 29. N is calculated according to equation (2) with the c_s selected is 0.6. Maximum flux density is 1.229 T for permanent magnet volume 160 mm² while minimum flux density is 1.14 T for permanent magnet volume is 320 mm². The entire model has the same point of flux density for the same permanent magnet volume.

2.3. Selection of Field Model for Conventional BLDC Motor

Figure 7 shows the final process for the structure design. The number of turn is set to the best value which is 29 and 6 A respectively. Flux density at stator pole will be recorded and analyze. The best model for BLDC motor will be selected and other analyzing process will be conducted.

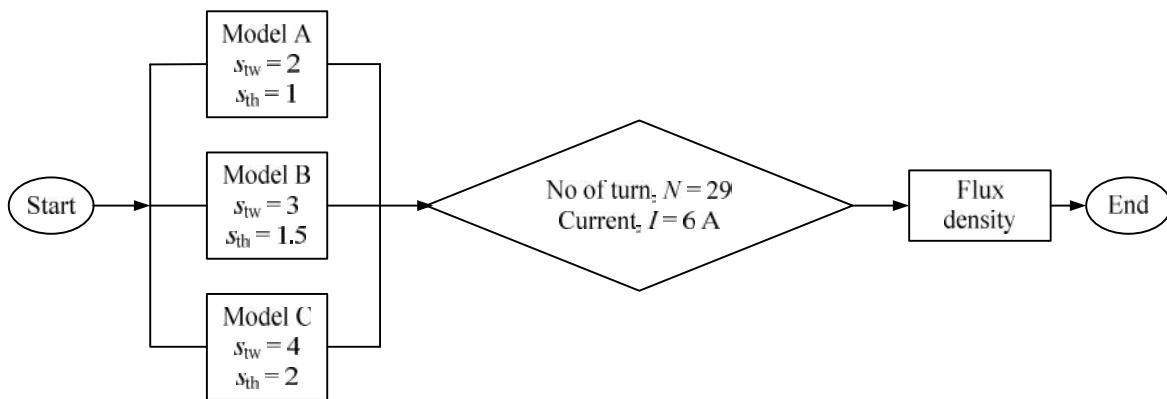


Figure 7. Selection of model

With the result from analysis for stator pole and permanent magnet volume, model B with magnet volume 320 mm² is chosen for design of BLDC motor and further analysis for back emf, flux linkage and torque for analyzing motor performance. Figure 8 (a) shows three-phase back emf, E for the conventional BLDC motor. The peak value of back emf is 1.04 V for all the three phases. Figure 8 (b) shows flux linkage of the conventional BLDC motor. The peak value of flux linkage is 2.3mWb. The graph for flux linkage is in positive cycle with time, t from 0 ms until 4 ms. Figure 8 (c) shows static torque waveform with the peak value of torque is 0.19 Nm. This waveform is simulated using DC current mode.

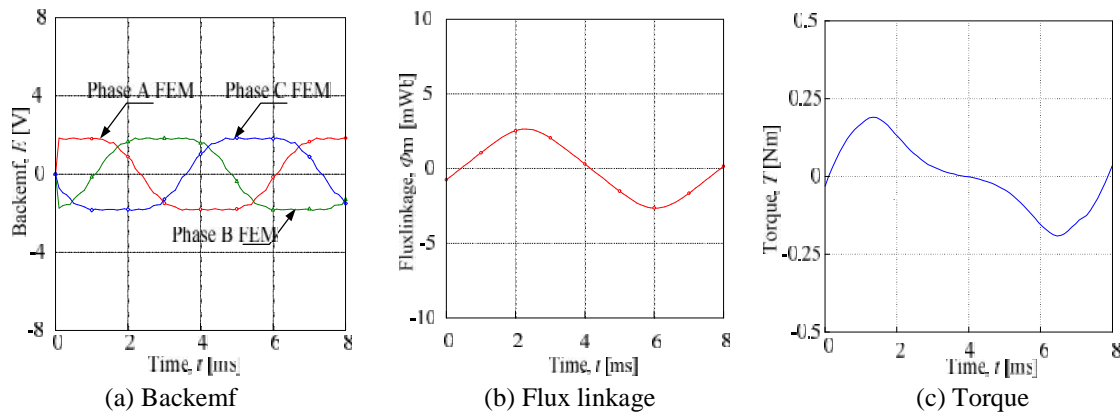


Figure 8. Final model analysis

3. DESIGN OF HOLLOW-ROTOR

After all the process for designing conventional BLDC motor is done, conventional BLDC motor is converted to hollow rotor by changing the magnet arrangement and replacing area below magnet completely with air. Figure 9 shows design of hollow-rotor. The basic structure of conventional BLDC motor is shown in Figure 9 (a). In this research, BLDC motor is designed for 9 slot 8 pole arrangements. The permanent magnet volume and coil turn is 320 mm^3 and 29 turns, respectively. The stack length and diameter of the BLDC is 40 mm and 50 mm, respectively. The rotor and stator is mostly covered by standard silicon steel grade as J1: 50H800. As rotor is covered by silicon steel material, it will influence flux of magnet to pass through the area below the ferromagnetic material. As a result, there is more leakage flux circling at the end of the permanent magnet. To reduce leakage at the end of permanent magnet, area below rotor is changed to hollow as shown in Figure 9 (b) known as hollow-rotor BLDC motor. The arrangement of magnet in a hollow-rotor is different with other BLDC motor where magnet is arranged to maximally reduce leakage flux. Hollow which consists of an air, has higher reluctance, thus channeling all flux to the nearest ferromagnetic material. In a hollow rotor spoke type BLDC motor, all flux will go around stator where it will maximize the usage of flux in the motor. Figure 9 (c) shows generated flux for conventional BLDC motor. As rotor is covered by silicon material, it will influence flux of magnet where most of magnetic flux passing through the area will pass near the ferromagnetic material. There is more leakage flux circling at the end of the permanent magnet thus less flux is being used in the air gap. Figure 9 (d) shows generated flux for hollow-rotor BLDC motor. The arrangement of magnet in a hollow-rotor is different with conventional BLDC motor where magnet is arranged to maximally reduce leakage flux. Hollow which consists of an air, has higher reluctance, thus channeling all flux to the nearest ferromagnetic material. In a hollow rotor spoke type BLDC motor, all flux will go around stator where it will maximize the usage of flux in the motor. Figure 9 (e) shows comparison torque by using FEM analysis for BLDC motor and hollow-rotor. When hollow-rotor is used, torque increases maximumly from 0.19 Nm to 0.39 Nm. For validation purpose, a prototype of rotor spoke BLDC motor is fabricated as shown in Figure 9 (f).

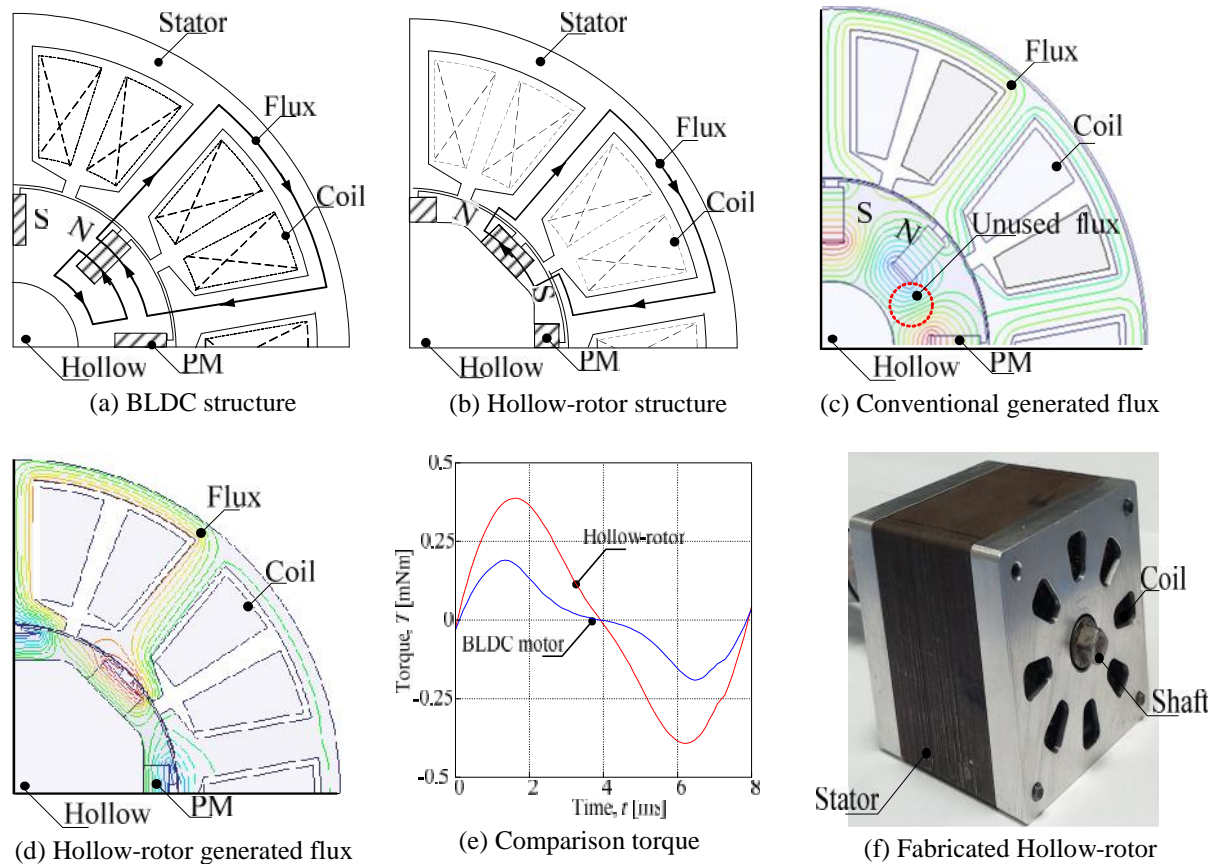


Figure 9. Design of Hollow-rotor

4. EXPERIMENTAL SETUP

To verify simulation result the static and dynamic torque measurement is carried out for the fabricated model. The static torque of the measurement result is compared with the simulation result. Meanwhile, the dynamic torque (torque and speed characteristic) of the measurement result also conducted. This experiment is to indicate maximum speed and torque when motor are operates.

4.1 Static Torque Characteristic

Figure 10 shows equipment setup for static torque experiment. After torque sensor had been calibrated, the handle is connected towards torque sensor. This handle will be rotated to rotate the gear and rotor shaft by 1:10. Shaft torque sensor is connected to fabricated motor and the gear. Current source is set for motor input current. Torque sensor is connected to dynamic strain amplifier which will amplify the output signal of the torque sensor which consists of measure torque, acceleration, load, pressure and others. Output of dynamic strain amplifier is connected to oscilloscope for data presentation. When handle is rotated in a positive and negative circle, torque will be produced. Data from oscilloscope will be saved into USB drive and analyze by using a laptop.

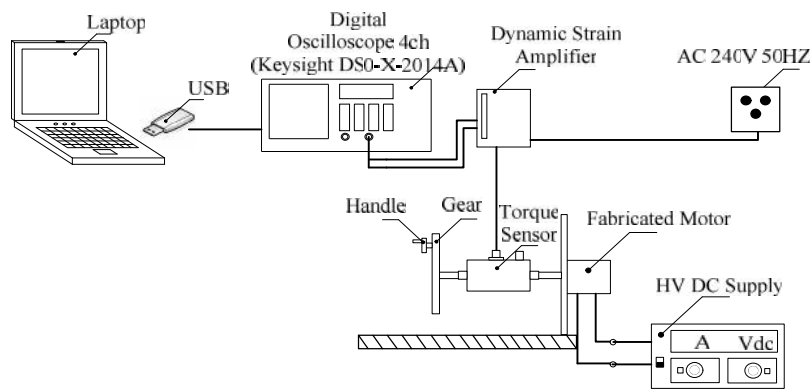


Figure 10. Equipment setup for static torque measurement

4.2 Torque And Speed Characteristic

Figure 11 shows diagram for torque and speed measurement setup. Speed sensor will measure the speed in rpm which will be shown by digital speed indicator. Torque sensor is connected to dynamic strain amplifier which allows the data to be presented in oscilloscope. For this experiment, a BLDC driver is used to operate hollow rotor BLDC motor.

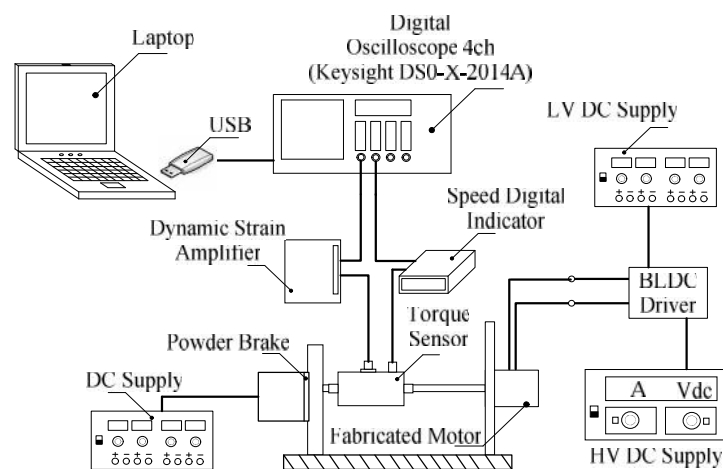


Figure 11. Torque and Speed measurement setup

Voltage 15 V is being supply to the BLDC driver to triggering the switching device (MOSFET). Voltage 5 V is set for supplying Hall Effect sensor, meanwhile the motor supply is set for 12 V. Then, for next experiment the supply is change to 24 V and 48 V. Three phase wye connection is set to BLDC driver. Powder brake is connected to torque sensor shaft. Other power supply is used for powder brake; the powder brake is being supply with 0.5 V, 1.0 V, 1.5 V and 2.0 V to provide different value of braking torque. Figure 11 shows measurement setup of torque and speed characteristic in the laboratory.

5. PERFORMANCE ANALYSIS OF HOLLOW-ROTOR

Figure 12 (a) shows back emf for hollow-rotor spoke type BLDC motor at speed of 1000 rpm. The maximum back emf for measurement for hollow-rotor motor is 4.5 V while for FEM simulation is 5V. Percentage difference for measurement and simulation is 10 %. Figure 12 (b) shows the static torque when the current of 6 A is applied at speed of 1000 rpm. The maximum value of torque during experiment is 0.28 Nm while the maximum value of torque using FEM simulation is 0.3 Nm. The percentage error between measurement and simulation is about 8 %. The dynamic torque is shown in Figure 12 (c). Measurement result is compared with FEM when current source is 6 A. The maximum torque for measurement is 0.15 Nm while maximum torque for simulation is 0.12 Nm. Figure 12 (d) shows the torque vs speed for hollow-rotor spoke type BLDC motor. Result is recorded for input voltage from 12 V to 48 V. The result from measurement is compared to FEM simulation for verification purpose. For 12 V measurements, the maximum torque is 0.29 Nm when speed is 500 rpm while the minimum torque is 0.167 Nm when speed is 1092 rpm. By using FEM simulation (12 V), the maximum torque is 0.31 Nm for 500 rpm while the minimum torque is 0.18 Nm for 1092 rpm. For 48 V measurements, the maximum torque is 0.459 for 900 rpm while the minimum torque is 0.375 Nm for 1722 rpm. For FEM, the maximum value of torque is 0.47 Nm when speed is 900 rpm while the minimum torque is 0.39 Nm for 1722 rpm. Percentage difference of the result for measurement compared with FEM simulation is 8 %. It can be seen that the torque is inversely proportional to the speed of BLDC motor.

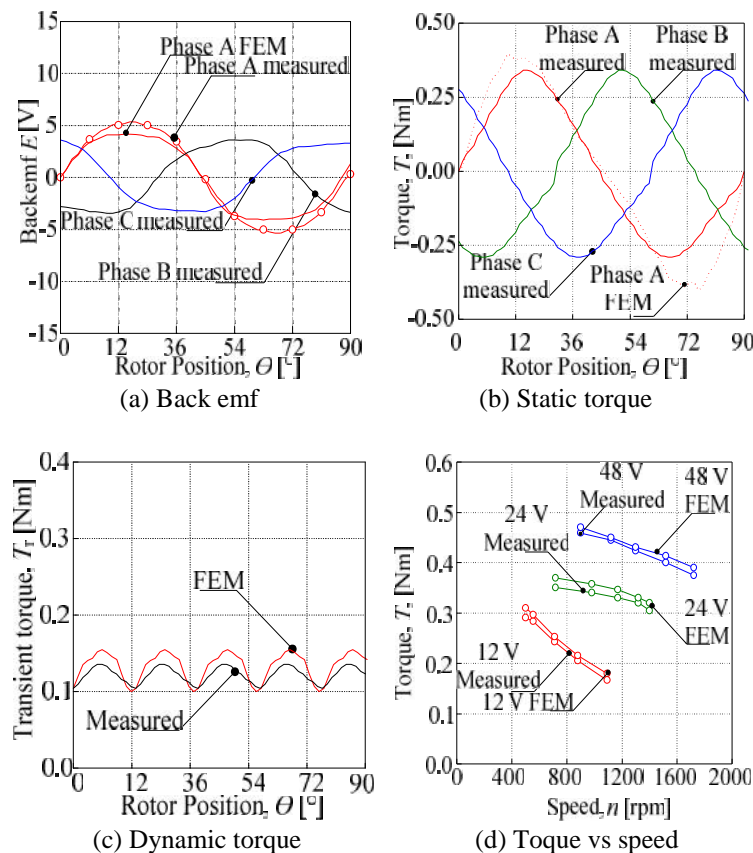


Figure 12. Hollow-rotor Analysis

6. CONCLUSION

In this paper, the design for hollow-rotor motor has been presented. In the beginning, conventional BLDC motor is designed, and then analysis process for choosing the right model with proper coil size is chosen. Based on the investigation one BLDC model with reasonable magnet volume is been selected and analyze in terms of back emf, flux linkage and torque before converted to hollow-rotor BLDC motor. A new model structure called hollow-rotor is proposed and result for torque is compared with BLDC motor where it shows increment of torque from 0.19 Nm to 0.39 Nm. For validation, a prototype of hollow rotor spoke BLDC motor had been fabricated. The percentage difference between simulation and measurement is 8 %. This shows that the simulation result has good agreement with the measurement result. As a conclusion, the hollow spoke type topology can be used in designing higher torque to weight ratio of motor.

ACKNOWLEDGEMENTS

The author would like to thank the Ministry of Higher Education, Universiti Teknikal Malaysia Melaka (UTeM) and Universiti Putra Malaysia (UPM) for providing the funding for the esearch under grant FRGS/1/2014/TK03/FKE/02/F00208 and RACE/F3/TK14/FKE/F00250.

REFERENCES

- [1] M.A.Salam., *Fundamental of Electrical Machines*. U.K: Oxford, 2005.
- [2] M.H.Rashid., *Power Electronic, 3rd Edition*. Pearson: Prentice Hall, 2004.
- [3] F.J.Gieras, W. Mitchell., *Permanent Magnet Motor Technology*, Ohio: Columbia, 2002.
- [4] A. Balakrishnan., *Electrical Machines-I*. Engineering series, Perpustakaan Negara Malaysia, 2008.
- [5] H.G. Kim, J.H., H.G. Sung, and J.P. Hong, "Optimal Design of Spoke Type BLDC Motor Considering Irreversible Demagnetization of Permanent Magnet," ICEMS 2003. *Sixth International Conference*, Vol 1 234-237, 2013.
- [6] H.G. Kim, J. Hur, W.B. Kim, G.H. Kang, "Irreversible Demagnetization Analysis of IPM type BLDC Motor Considering the Circulating Current by Stator Turn fault", *Electromagnetic Field Computation (CEFC), 2010 14th Biennial IEEE Conference*, 2013.
- [7] G.H. Kang, H. Hur, "Analysis of Irreversible Magnet Demagnetization in Line-Start Motors Based on the Finite-Element Method", *Transactions on Magnetics*, Vol. 39.No. 4, 1488-1491, May 2003.
- [8] B.K. Lee, G.H. Kang, J. Hur, and D. W. You, "Design of Spoke Type BLDC Motors with High Power Density for Traction Applications", *Industry Applications Cobference*, Vol 2 1068-1072, 2004.
- [9] S.J. Salon, *Finite Element Analysis of Electrical Machines*, Rensselaer Polytechnic Institute, Troy, New York, 1995.
- [10] G.H. Kang, J.P. Hong, J.P. Kim, and J.W. Park, "Improved Parameters Modeling of Interior Permanent Magnet Synchronous Motor by Finite Element Analysis", *IEEE Transactions on Magnetics*, Vol.36, no.4, 1867-1870, 2000.
- [11] M.R. Mohammad, K.T. Kim, and J. Hur, "Design and Analysis of a Spoke Type Motor With Segmented Pushing Permanent Magnet for Concentrating Air-Gap Flux Density", *IEEE Transactions on Magnetics*, Vol. 49, no. 5 2397-2400,2013.
- [12] M.R. Mohammad, K.T. Kim, and J. Hur, "Design and Analysis of Neodymium free Spoke Type Motor with Segmented Wing Shape Permanent Magnet for Concentrating Flux Density", *Energy Conversion Congress and Exposition (ECCE)*, 4991-4997, 2013.
- [13] H.W. Kim, K.T. Kim, Y.S. Jo, and J. Hur, "Optimization Methods of Torque Density for Developing the Neodymium Free Spoke Type BLDC Motor", *IEEE Transactions on Magnetics*, Vol 49 2173-2176, 2013.

BIOGRAPHIES OF AUTHORS



R. N. Firdaus was born on May 1982 at Parit Buntar, Perak, Malaysia. He received B. Eng., M.Sc. and Ph.D. in Electrical Power Engineering from Universiti Putra Malaysia. In 2006, 2009 and 2013, respectively. He is currently senior lecturer in Department of Power Electronics and Drives, Faculty of Electrical Engineering, Universiti Teknikal Malaysia Melaka. His research interest includes applied magnetics, electrical machines, magnetic sensor and drives.



S. Farina was born on 14 April 1987 at Malacca, Malaysia. In 2007, she received Diploma in Electrical and Electronic from Infrastructure University Kuala Lumpur (IUKL). In 2012, she received her B. Eng., from Universiti Teknikal Malaysia Melaka (UTeM). Currently, she is pursuing her study in M.Sc. in Electrical Engineering from the same university. Her research study is machine design.



R. Suhairi was born on 13 June 1984 at Kota Baru Kelantan. He received the B. Eng. in Industrial Electronics from Universiti Malaysia Perlis, Malaysia in 2009, and M. Sc. degrees in Electrical Power Engineering from Universiti Putra Malaysia, Malaysia in 2012. Currently he is pursuing his Ph. D. in electrical machine design at Universiti Teknikal Malaysia Melaka. His research interests are electrical machine design, electric machine simulation, electric drives, energy conversion, and renewable energy.



K. A. Karim received the M.Sc. from University of Bradford and Ph. D. degrees from the University of Nottingham, UK, in 2003 and 2011, respectively. He is currently a Senior Lecturer with the Department of Power Electronics and Drives, Faculty of Electrical Engineering, Universiti Teknikal Malaysia Melaka, Durian Tunggal, Malaysia. His research interests include electrical machine design, power electronics, and electric vehicle.



A. Jidin received the B. Eng., M. Sc. in power electronics and drives and Ph. D in electrical engineering from Universiti Teknologi Malaysia, Johor Bahru, Malaysia, in 2002, 2004, and 2011 respectively. He is currently a Lecturer with the Department of Power Electronics and Drives, Faculty of Electrical Engineering, Universiti Teknikal Malaysia Melaka, Durian Tunggal, Malaysia. His research interests include the field of power electronics, motor drive systems, field-programmable gate array, and DSP applications.



T. Sutikno received the B. Eng. degree in electrical engineering from Diponegoro University, Semarang, Indonesia, in 1999; the M. Eng. in electrical engineering from Gadjah Mada University, Yogyakarta, Indonesia, in 2004 and Ph.D. in electrical engineering from Universiti Teknologi Malaysia, Johor Bahru, Malaysia, in 2016. Since 2001, he has been a Lecturer with the Department of Electrical Engineering, Faculty of Industrial Technology, Universitas Ahmad Dahlan, Yogyakarta, Indonesia; and since 2008 he is an Associate Professor. His research interests include the field of power electronics, motor drive systems and field-programmable gate array applications



M. Norhisam received B. Eng, M. Sc. and Ph. D from Shinshu University Japan in 1998, 2000 and 2003, respectively. He is currently an Assoc. Prof at Department of Electrical and Electronic, Faculty of Engineering, Universiti Putra Malaysia. His area of interest is applies magnetic, magnetic sensor, electrical motor design, electrical generator design and power electronic.